



**HAL**  
open science

## Identification of salicylic acid-independent responses in an *Arabidopsis* 3 phosphatidylinositol 4-kinase beta double mutant

Tetiana Kalachova, Martin Janda, Vladimír Šašek, Jitka Ortmannová, Pavla Nováková, Petre I Dobrev, Volodymyr Kravets, Anne Guivarc'H, Deborah Moura, Lenka Burketová, et al.

### ► To cite this version:

Tetiana Kalachova, Martin Janda, Vladimír Šašek, Jitka Ortmannová, Pavla Nováková, et al.. Identification of salicylic acid-independent responses in an *Arabidopsis* 3 phosphatidylinositol 4-kinase beta double mutant. *Annals of Botany*, 2020, 125 (5), pp.775-784. 10.1093/aob/mcz112 . hal-02163223

**HAL Id: hal-02163223**

**<https://hal.science/hal-02163223>**

Submitted on 24 Jun 2019

**HAL** is a multi-disciplinary open access archive for the deposit and dissemination of scientific research documents, whether they are published or not. The documents may come from teaching and research institutions in France or abroad, or from public or private research centers.

L'archive ouverte pluridisciplinaire **HAL**, est destinée au dépôt et à la diffusion de documents scientifiques de niveau recherche, publiés ou non, émanant des établissements d'enseignement et de recherche français ou étrangers, des laboratoires publics ou privés.

1 Original Article

2

3 **Identification of salicylic acid-independent responses in an Arabidopsis**  
4 **phosphatidylinositol 4-kinase beta double mutant**

5

6 KALACHOVA<sup>+</sup> Tetiana<sup>1,5</sup>, JANDA<sup>+</sup> Martin<sup>1,2</sup>, ŠAŠEK Vladimír<sup>1</sup>, ORTMANNOVÁ Jitka<sup>1,6</sup>,  
7 NOVÁKOVÁ Pavla<sup>1,2</sup>, DOBREV I. Petre<sup>1</sup>, KRAVETS Volodymyr<sup>3</sup>, GUIVARC'H Anne<sup>4</sup>,  
8 MOURA Deborah<sup>5</sup>, BURKETOVÁ Lenka<sup>1</sup>, VALENTOVÁ Olga<sup>2</sup>, RUELLAND Eric<sup>4,5\*</sup>

9

10 <sup>1</sup>Institute of Experimental Botany, The Czech Academy of Sciences, Prague 160 000, CZECH  
11 REPUBLIC

12 <sup>2</sup>University of Chemistry and Technology, Department of Biochemistry and Microbiology,  
13 Prague 166 28, CZECH REPUBLIC

14 <sup>3</sup>Institute of Bioorganic Chemistry and Petrochemistry National Academy of Sciences of  
15 Ukraine, 02094 Kyiv, UKRAINE

16 <sup>4</sup>CNRS, Institut d'Ecologie et des Sciences de l'Environnement de Paris, UMR 7618, Créteil,  
17 FRANCE

18 <sup>5</sup>Université Paris-Est, UPEC, Institut d'Ecologie et des Sciences de l'Environnement de Paris,  
19 Créteil, FRANCE

20 <sup>6</sup> current address - Department of Plant Biology, Swedish University of Agricultural Sciences,  
21 SE-750 07 Uppsala, SWEDEN

22

23 **Running title: Salicylic acid-independent responses in PI4K mutants**

24 \* Corresponding author: Eric RUELLAND e-mail address: [eric.ruelland@upmc.fr](mailto:eric.ruelland@upmc.fr)

25 <sup>+</sup> Equally contributed

26 **Abstract**

27

28 **Background and Aims**

29 We have recently shown that an *Arabidopsis thaliana* double mutant of type III  
30 phosphatidylinositol-4-kinases (PI4Ks), *pi4kβ1β2*, constitutively accumulated a high level of  
31 salicylic acid (SA). By crossing this *pi4kβ1β2* double mutant with mutants impaired in SA  
32 synthesis (such as *sid2* impaired in isochorismate synthase) or transduction, we demonstrated  
33 that the high SA level was responsible for the dwarfism phenotype of the double mutant. Here  
34 we aimed at distinguishing between the SA-dependent and -independent effects triggered by  
35 the deficiency in *PI4Kβ1* and *PI4Kβ2*.

36 **Methods**

37 To achieve this, the *sid2pi4kβ1β2* triple mutant was a tool of choice. High-throughput  
38 analyses of phytohormones were performed on this mutant together with *pi4kβ1β2* and *sid2*  
39 mutants and wild-type plants. Responses to pathogens, namely *Hyaloperonospora*  
40 *arabidopsidis*, *Pseudomonas syringae* and *Botrytis cinerea*, but as well to the non-host fungus  
41 *Blumeria graminis*, were also determined. Callose accumulation was monitored in response to  
42 flagellin.

43 **Key Results**

44 We show here the prominent role of high SA levels in influencing the concentration of many  
45 other tested phytohormones, including abscisic acid and its derivatives, the Aspartate-  
46 conjugated form of indole-3-acetic acid and some cytokinins such as *cis*-zeatin. We show that  
47 the increased resistance of *pi4kβ1β2* plants to the host pathogens *Hyaloperonospora*  
48 *arabidopsidis*, *Pseudomonas syringae* pv. *tomato* DC3000 and *Bothrytis cinerea* is dependent  
49 on accumulation of high SA level. In contrast, accumulation of callose in *pi4kβ1β2* after

50 flagellin treatment was independent of SA. Concerning the response to *Blumeria graminis*,  
51 both callose accumulation and fungal penetration were enhanced in the *pi4kβ1β2* double  
52 mutant compared to wild-type plants. Both of these processes occurred in a SA-independent  
53 manner.

#### 54 **Conclusions**

55 Our data extensively illustrate the influence of SA on other phytohormone levels. The  
56 *sid2pi4kβ1β2* triple mutant allowed to uncover the role of PI4Kβ1/β2 *per se*, thus showing the  
57 importance of these enzymes in plant defence responses.

58

59 **Key words:** pi4kβ1β2 / PI4Ks, callose, salicylic acid, phytohormones, isochorismate synthase  
60 1, biotic stress, pathogens, *Arabidopsis thaliana*

61

62

## 63 INTRODUCTION

64 Salicylic acid (SA) is a phytohormone playing a role in many plant physiological processes  
65 although its role is mainly documented in plant response to biotic stress when SA accumulates  
66 within tissues, both at the site of attack and in a systemic manner (Vlot et al. 2009; Janda  
67 2015). In plants, SA is biosynthesized via two pathways. One is dependent on phenylalanine  
68 ammonia-lyase (PAL; EC 4.3.1.24) which catalyses the conversion of phenylalanine to *trans*-  
69 cinnamic acid. In the other pathway, the key enzyme is ISOCHORISMATE SYNTHASE  
70 (ICS; EC 5.4.4.2) which catalyses the isomerization of chorismate into isochorismate  
71 (Dempsey et al. 2011). The ICS-dependent pathway was shown to be responsible for most SA  
72 accumulation upon pathogen attack. In *A. thaliana*, two ICS isoforms exist, but the major role  
73 in SA biosynthesis is played by ICS1. The *ICS1* mutant is known as *sid2* for *salicylic acid*  
74 *induction deficient 2* (Wildermuth et al. 2001; Wagner et al. 2013; Cui et al. 2017). When SA  
75 levels increase, downstream signalling events are triggered, and the best described molecular  
76 pathway is dependent on NONEXPRESSOR OF PATHOGENESIS RELATED 1 (NPR1).  
77 Upon SA action, homo-oligomeric NPR1 protein undergoes dissociation by reduction and the  
78 resulting monomers move into the nucleus where they interact with TGA-transcription factors  
79 to induce the expression of SA responsive genes. A NPR1 independent pathway also exists in  
80 response to SA (Janda 2015). The activation of SA signalling pathways leads to robust  
81 changes in the plant transcriptome, including defence related genes (Seyfferth and Tsuda  
82 2014). Among the immune responses affected by changes in SA levels or by SA treatments is  
83 the accumulation of callose (Antignani et al. 2015; Dong et al. 2008; Kohler et al. 2002), a  
84 (1,3)- $\beta$ -Glucan occurring in plant cell walls.

85 The signaling pathways triggered by SA are still the subject of current research. We have  
86 shown that phosphoinositides, the phosphorylated derivatives of phosphatidylinositol (PI), are  
87 involved in SA transduction. Indeed, PI can be phosphorylated at the D4 position of the

88 inositol ring by phosphatidylinositol-4-kinases (PI4K) thus leading to phosphatidylinositol 4-  
89 phosphate (PI4P); which can be phosphorylated further into phosphatidylinositol-4,5-  
90 bisphosphate (PI-4,5-P<sub>2</sub>). There are two types of PI4Ks according to their primary sequences  
91 and pharmacological sensitivities. Type II PI4Ks are inhibited by adenosine while type III  
92 PI4Ks are inhibited by micromolar concentrations of wortmannin, a steroid metabolite  
93 produced by the fungus *Penicillium funiculosum* (Nakanishi et al. 1995, Balla 2007, Krinke et  
94 al. 2007). From the *A. thaliana* genome, twelve putative PI4K isoforms have been identified.  
95 Eight belong to type-II (AtPI4K $\gamma$ 1-8), and four belong to type-III (AtPI4K $\alpha$ 1 and  $\alpha$ 2,  
96 AtPI4K $\beta$ 1 and  $\beta$ 2) (Delage et al. 2012; Janda et al. 2013). We have shown that type III-PI4Ks  
97 are activated when *A. thaliana* suspension cells respond to SA, thus leading to an increase in  
98 PI4P and PI-4,5-P<sub>2</sub> (Krinke et al. 2007). PI-4,5-P<sub>2</sub> can act as a cofactor to some phospholipase  
99 Ds (Pappan et al. 1998). Interestingly, there is an overlap between SA responsive genes  
100 controlled by PI4Ks and those controlled by PLDs, leading to the working model that in  
101 response to SA, PI4P and PI-4,5-P<sub>2</sub> are produced with PI-4,5-P<sub>2</sub> acting as a cofactor for a  
102 PLD, whose product, PA, will trigger a signalling cascade (Krinke et al. 2009; Kalachova et  
103 al. 2016).

104 In order to better characterize the role of PI4Ks in the response to SA, we have used *A.*  
105 *thaliana* mutants altered in type III PI4Ks. We previously worked on a double mutant  
106 defective in the two PI4K $\beta$  genes. Surprisingly, *pi4k $\beta$ 1 $\beta$ 2* exhibited a constitutively high SA  
107 level that resulted in constitutive high transcription of SA responsive genes such as *PR-1*  
108 (PATHOGENESIS RELATED 1). Therefore, PI4Ks are not only involved in SA transduction  
109 but they can also impact SA concentration. Furthermore, this double mutant exhibited  
110 dwarfism and was more resistant to the bacterial pathogen *Pseudomonas syringae* pv.  
111 *maculicola* ES4326 (Sasek et al. 2014). The *pi4k $\beta$ 1 $\beta$ 2* plant was crossed with mutants  
112 impaired in components of SA synthesis (*sid2*, impaired in *ICS1* expression; *eds1*), SA

113 transduction (*npr1*) or a mutant expressing bacterial SA-hydroxylase (NahG) that degrades  
114 SA to catechol. The resulting triple mutants allowed us to conclude that the dwarf phenotype  
115 of *pi4kβ1β2* plants was dependent on SA accumulation and its transduction *via* the NPR1  
116 pathway (Janda et al. 2014; Sasek et al. 2014).

117 In the present study, our aim was to identify amongst the cellular and physiological processes  
118 affected by the deficiency of PI4Kβ1β2, those that were either SA-dependent or SA-  
119 independent. To achieve this, we used the *sid2pi4kβ1β2* triple mutant that does not  
120 accumulate SA and exhibits wild-type sized rosettes (Sasek et al. 2014). In this mutant, the  
121 effects of PI4Kβ1 and PI4Kβ2 mutations would not be masked by high SA levels. We showed  
122 that hormonal levels and pathogen resistance were mainly dependent on SA. However, we  
123 could show that *sid2pi4kβ1β2* plants accumulated higher amounts of callose in response to  
124 *flg22* and wounding. Interestingly, this SA-independent callose accumulation was also  
125 observed during early stages of interactions with *Blumeria graminis* when penetration was  
126 observed. Our data suggest that PI4Ks are involved in plant immune responses not only  
127 through SA accumulation but also via SA-independent processes.

128

## 129 **MATERIALS AND METHODS**

130

### 131 **Plant material, growth conditions**

132 In this study, we used the following genotypes of *A. thaliana*: Columbia-0 (WT), *sid2-3*  
133 (Gross et al. 2006), *npr1-1* (Cao et al. 1997) *NahG* (Delaney et al. 1994), *pi4kβ1β2*  
134 (SALK\_040479 / SALK\_09069; Preuss et al. 2006), *sid2pi4kβ1β2*, *NahGpi4kβ1β2*, and  
135 *npr1pi4kβ1β2* mutants previously described (Sasek et al. 2014).

136 All plants were cultivated in Jiffy 7 peat pellets at 22°C with 70% relative humidity. All  
137 plants were watered without additional fertilizers. As for the light regimes, plants were

138 routinely cultivated in daily cycles of 10 h light (100-130  $\mu\text{E m}^{-2} \text{s}^{-1}$ ) and 14 h dark. Plants  
139 that would be used for hormonal analysis or transcription analysis were cultivated under 16 h  
140 light (130-150  $\mu\text{E m}^{-2} \text{s}^{-1}$ ) and 8 h dark.

#### 141 Pathogen **inoculation**

142 Two-week-old plants grown at high density in one pot were sprayed with *H. arabidopsidis*  
143 *NoCo2* spores (~100 spores/ $\mu\text{l}$ ). The infected plants were cultivated in closed transparent plastic  
144 boxes in high humidity for 6 days under 16 h light/8 h dark (100-130  $\mu\text{E m}^{-2} \text{s}^{-1}$ ) at 19°C. For  
145 analysis, leaves collected from one pot were considered as one sample (for each genotype, 11  
146 samples were analysed). Spores were counted under a microscope using a Bürker chamber and  
147 expressed as relative spore number in [%], where relative spore number for a given control  
148 genotype (WT or *sid2*) was set to 100%. The spores were counted as spores per mg of tissue fresh  
149 weight. The experiments [WT vs *pi4k $\beta$ 1 $\beta$ 2*] and [*sid2* vs *sid2pi4k $\beta$ 1 $\beta$ 2*] were conducted  
150 independently.

151 Inoculation with *Pseudomonas syringae* was performed according to (Katagiri et al. 2002)  
152 with modifications. Bacteria were cultivated overnight on King's B medium plates containing  
153 rifampicin (50  $\mu\text{g}/\mu\text{l}$ ). *Pseudomonas syringae* pv. *tomato* DC3000 (*Pst* DC3000) and  
154 *Pseudomonas syringae* pv. *tomato* DC3000 AvrRpt2 (*Pst* DC3000 AvrRpt2) were taken from  
155 the respective plate and resuspended in 10mM  $\text{MgCl}_2$  to give an  $\text{OD}_{600}=0.001$ . Four-week-old  
156 plants were infiltrated with this suspension.

157 One disc (6 mm) from one leaf, three leaves at a similar developmental stage from one plant  
158 and three plants were collected as one sample of one genotype at 0 dpi and 3 dpi (3 dpi only  
159 for *Pst* DC3000; 2 dpi for *Pst* DC3000 AvrRpt2). Leaf discs were ground in 10mM  $\text{MgCl}_2$   
160 and decimal dilutions were performed. Colony forming units were counted.

161 Four-week-old *A. thaliana* plants were treated with 6  $\mu\text{l}$  drops containing *Botrytis cinerea*  
162 BMM spores ( $5 \cdot 10^4$  spores/ml) by applying a single drop to each leaf, with three leaves at a



163 similar developmental stage inoculated for each plant. Treated plants were placed into closed  
164 plastic boxes and kept in low light (16h light/8h dark, 21°C; 10-20  $\mu\text{E m}^{-2} \text{s}^{-1}$ ) for 56 hpi.  
165 *Blumeria graminis* f. sp. *hordei* (*Bgh*) was cultivated continuously on fresh barley (Golden  
166 promise) grown under short day conditions (19°C, 10/14 h, 50% humidity, at a light intensity  
167 of 70  $\mu\text{mol m}^{-2} \text{s}^{-1}$ ). Plants, approximately 4 weeks old, were inoculated by spreading spores  
168 from infected barley onto the adaxial side of their leaves (from leaf to leaf). The 5th - 6th  
169 leaves were cut off at selected hpi and cleared with 96% ethanol or chloral hydrate. For  
170 penetration rate, fungal structures were stained with 250 mg/ml trypan blue in a  
171 lactophenol/ethanol solution (Vogel and Somerville 2000). Stained leaves were observed by  
172 classical epifluorescence microscopy or bright-field microscopy using a Zeiss AxioImager  
173 ApoTome2 (objective 100x).

174

#### 175 **Callose deposition**

176 Four-week-old *A. thaliana* plants were treated for 24 h with 100 nM flg22 or infiltrated with  
177 *Pst DC3000*. Distilled water infiltration was used as a control (mock) treatment. Infiltrated  
178 leaves were decolorized in ethanol:glacial acetic acid (3:1 v/v). The leaves were then rehydrated  
179 in successive baths of 70% ethanol (at least 1 h), 50% ethanol (at least 1 h), 30% ethanol (at  
180 least 1 h) and water (at least 2h). Leaves were stained for 4 h with 0.01 % aniline blue in 150  
181 mM  $\text{K}_2\text{HPO}_4$ , pH 9.5. Callose deposition was observed by fluorescence microscopy using a  
182 Zeiss AxioImager ApoTome2 (objective 10x). In the case of *Bgh* infection analysis, we  
183 calculated only callose spots using the high circularity function of the measurement settings at  
184 an interval of 0.5-1 which allowed us to distinguish only the cells with the size exclusion limit  
185 for spots corresponding to either encased haustoria or enormous papilla. Callose deposition  
186 was observed by fluorescence microscopy using a Zeiss AxioImager ApoTome2 (objective

187 10x). Images were processed with ImageJ software. At least four leaves from three  
188 independent plants were analysed for each variant.

189

### 190 **RNA extraction and qPCR analysis**

191 Plant tissues were homogenised in 2-ml screw-cap tubes containing 1 g of 1.3-mm diameter  
192 silica beads using a FastPrep-24 instrument (MP Biomedicals, Santa Ana, CA, USA). Total  
193 RNA was isolated using a Spectrum Plant Total RNA kit (Sigma-Aldrich, USA) and treated  
194 with a DNA-free kit (Ambion, USA). Subsequently, 1 µg of RNA was converted to cDNA  
195 with M-MLV RNase H-Point Mutant reverse transcriptase (Promega Corp., USA) and an  
196 anchored oligo dT21 primer (Metabion, Germany). Gene transcription was quantified by  
197 qPCR using a LightCycler 480 SYBR Green I Master kit and a LightCycler 480 (Roche,  
198 Switzerland). The PCR conditions employed were 95°C for 10 min followed by 45 cycles of  
199 95°C for 10 s, 55°C for 20 s, and 72°C for 20 s. Melting curve analyses were then carried out.  
200 Relative transcription was normalized to the housekeeping genes *SAND* or *TIP41*  
201 (Czechowski et al. 2005). Primers were designed using PerlPrimer v1.1.21 (Marshall, 2004).  
202 The primers used were CalS1\_FP, AAGAGCGGAGGGTCACTTTG;  
203 CalS1\_RP, GGCGACACGAATAGACGGAT; CalS12\_FP,  
204 TTTACTCCGTTTTCCCGAGG; CalS12\_RP, GGAGAGAGACGCATCTGAGC.

205

### 206 **Analysis of plant hormones**

207 Plant hormones were extracted from 100 mg of frozen tissues and their concentrations were  
208 determined as previously described (Dobrev and Vankova 2012; Dobrev and Kaminek 2002)  
209 after the addition of appropriate internal standards. Hormone analysis was carried out on four  
210 samples, each taken from three plants. Briefly, samples were homogenized in tubes with 1.3  
211 mm silica beads using a FastPrep-24 instrument (MP Biomedicals, USA). Samples were then

212 extracted with a methanol/H<sub>2</sub>O/formic acid (15:4:1, v:v:v) mixture, which was supplemented  
213 with stable isotope-labeled phytohormone internal standards (10 pmol per sample) in order to  
214 check recovery during purification and to validate the quantification. The clarified  
215 supernatants were subjected to solid phase extraction using Oasis MCX cartridges (Waters  
216 Co., USA). The eluates were evaporated to dryness and the generated solids were dissolved in  
217 30 µl of 15% (v/v) acetonitrile in water. Hormones were separated and quantified by Ultimate  
218 3000 high-performance liquid chromatography (Dionex, Bannockburn, IL, USA) coupled to a  
219 3200 Q TRAP hybrid triple quadrupole/linear ion trap mass spectrometer (Applied  
220 Biosystems, Foster City, CA, USA) as described by (Dobrev et al. 2017). Metabolite levels  
221 were expressed in pmol/g fresh weight (FW).

222

### 223 **Statistical analysis**

224 At least three independent biological replicates were performed for all experiments. Statistical  
225 analysis was conducted by paired *t*-test or ANOVA with Tukey honestly significant  
226 difference (HSD) multiple mean comparison *post hoc* test. The number of analysed samples  
227 was specified for each condition. The correlation matrix for hormonal levels was prepared  
228 using R-software *Hmisc* and *corrplot* packages based on the Pearson correlation (Team 2014).

229

## 230 **RESULTS**

231

### 232 ***The pi4kβ1β2 double mutant has altered phytohormonal levels***

233 Our goal was to identify SA-dependent and SA-independent processes triggered by the double  
234 *pi4kβ1β2* mutation. To do so, we used a *sid2pi4kβ1β2* triple mutant. If a process triggered by  
235 the double *pi4kβ1β2* mutation is SA-dependent, then it should disappear in the *sid2pi4kβ1β2*

236 triple mutant. On the other hand, if a process triggered by the double *pi4kβ1β2* mutation is  
237 SA-independent, then it should still be observed in the *sid2pi4kβ1β2* triple mutant.

238 Since the main effect of the double *pi4kβ1β2* mutation was on the level of SA, we decided to  
239 quantify a broad spectrum of phytohormones in the *sid2pi4kβ1β2* triple mutant. The hormone  
240 levels obtained were compared to those of *pi4kβ1β2*, *sid2* and WT plants. A first look allowed  
241 us to establish that the *pi4kβ1β2* double mutation does not impact only SA levels. Many  
242 hormone-related metabolites showed significantly different levels in *pi4kβ1β2* plants when  
243 compared to WT plants while most of them remained at WT levels in *sid2pi4kβ1β2*  
244 (supplemental Table S1). In our previous study, we created an additional triple mutant by  
245 crossing *pi4kβ1β2* with a *NahG* mutant impaired in SA accumulation: *NahGpi4kβ1β2* (Sasek  
246 et al. 2014). To confirm and to strengthen the results obtained with *sid2pi4kβ1β2*, we also  
247 quantified phytohormones in *NahGpi4kβ1β2*, together with their corresponding single  
248 mutants (Supplemental table S1). From these data, we built a correlation matrix (Fig. 1).  
249 Many hormone levels were correlated to higher SA levels (Pearson correlation higher than  
250 0.7) as seen for the abscisic acid (ABA) derivatives such as 9-hydroxy-ABA (9OH-ABA),  
251 phaseic acid (PA) and dihydrophaseic acid (DPA). However, the high levels of DPA, PA and  
252 9OH-ABA observed in *pi4kβ1β2* versus WT were no longer seen in the triple mutants with  
253 low SA; therefore, these metabolite levels were controlled by SA in the *pi4kβ1β2* double  
254 mutant (Fig. S1A).

255 Since the main genetic pathway of SA response is controlled by NPR1, we investigated  
256 whether the hormonal control of SA was NPR1-dependent. This was achieved using a  
257 previously generated *npr1pi4kβ1β2* triple mutant where the SA level was 30-fold that of WT  
258 and 4-fold that of *pi4kβ1β2*. Interestingly, levels of DPA, PA and 9-OH were still high in  
259 *npr1pi4kβ1β2*, showing that the SA effect on these metabolites was only partially NPR1-  
260 dependent. It should be noted that ABA levels did not correlate with SA (Pearson correlation

261 0.3), thus indicating that the action of SA on ABA-derivatives is probably not directly  
262 connected with the biosynthesis of ABA, but with its metabolism.

263

264 Other hormones with high Pearson correlations to SA were the Asp conjugated form of  
265 indole-3-acetic acid (Asp-IAA) and some cytokinins. The increased level of IAA-Asp  
266 observed in *pi4kβ1β2* was no longer observed in the triple mutants with low SA. However, it  
267 was still visible in the *npr1pi4kβ1β2* triple mutant thus suggesting that this metabolite is  
268 controlled by SA but it is only partially NPR1-independent (Fig. S1B). The pattern of IAA  
269 was different from that of Asp-IAA, suggesting that SA control of Asp-IAA is on aspartate  
270 conjugation. As for cytokinins, the increase in *cis*-zeatin (*cZ*), *cis*-zeatin-riboside (*cZR*), *cis*-  
271 zeatin-7-N-glucoside (*cZ7G*), *cis*-zeatin-riboside-*O*-glucoside (*cZROG*) and *trans*-zeatin-*O*-  
272 glucoside (*tZOG*) and the decrease of *trans*-zeatin-7-N-glucoside (*tZ7G*) and *trans*-zeatin -9-  
273 N-glucoside (*tZ9G*) in the *pi4kβ1β2* double mutant was SA-driven. In contrast to the other  
274 hormones tested, SA action on *tZROG* appeared to be partially independent of NPR1 (Fig.  
275 S1C).

276

277 We identified one hormone for which its level was altered in *pi4kβ1β2* plants independently  
278 of SA. Indeed, the increase of oxIAA-GE observed in *pi4kβ1β2* was still visible in the triple  
279 mutants with low SA. It should be noted that oxIAA did not follow the same pattern (Fig. S2).

280

281

## 282 **Pathogen resistance, including a necrotroph, of *pi4kβ1β2* plants is SA-dependent**

283

284 At the hormonal level our data show that the major change induced by the *pi4kβ1β2* double  
285 mutation was an increase in SA, with this change determining the levels of many other

286 hormones. Since a major role of SA is related to biotic stress responses, we reasoned that  
287 processes related to biotic stress, dependent or not on SA, might also be altered in the double  
288 mutant.

289 Whether the PI4K double mutation *per se* was accompanied by an enhanced resistance to  
290 pathogens was investigated. Comparing resistance in *sid2pi4kβ1β2* plants to that in *pi4kβ1β2*  
291 or *sid2* would allow us to distinguish between the effectiveness of SA-dependent and  
292 independent responses. Therefore, different pathogens with different lifestyles (biotrophs,  
293 hemibiotrophs and necrotrophs) were tested (Glazebrook 2005). The *pi4kβ1β2* double mutant  
294 plants were more resistant to the biotroph *H. arabidopsidis* *NoCo2* compared to WT.  
295 However, *sid2pi4kβ1β2* resistance was similar to that of *sid2* plants (Fig. 2A). We then  
296 studied resistance to the hemibiotroph *Pseudomonas syringae* pv. *tomato* DC3000 in its wild  
297 type (*Pst* DC3000) or AvrRpt2 expressing form (*Pst* DC3000 AvrRpt2). *Pst* DC3000  
298 AvrRpt2 leads to a strong effector triggered immunity (ETI) response compared to *Pst*  
299 DC3000. With both forms, pathogen development was reduced in *pi4kβ1β2* plants compared  
300 to the WT while *sid2pi4kβ1β2* resistance was comparable to that of *sid2* and lower than WT  
301 plants (Fig. 2B, Fig. S3). Unexpectedly, the double mutant also showed an increased  
302 resistance to the necrotroph *B. cinerea* which was also SA-dependent since *sid2pi4kβ1β2*  
303 resistance was similar to that of *sid2* and WT plants (Fig. 2C). For each pathogenic assay,  
304 triple mutant resistance was similar to *sid2*, indicating that SA-dependent pathways were  
305 dominant in the immune response. Putative mechanisms regulated by PI4K activity alone  
306 were not sufficient to establish pathogen resistance.

307

308 **The enhanced level of basal callose deposition in *pi4kβ1β2* is mainly SA-dependent while**  
309 **stress-induced callose accumulation is not**

310 SA levels modulate numerous processes associated with immune responses including the  
311 strengthening of leaf tissues and particularly cell walls around the infection site by  
312 lignification and callose accumulation (Voigt 2014). Interestingly, SA pre-treatment also has a  
313 positive effect on flagellin-induced callose accumulation (Yi et al. 2014). We therefore  
314 studied callose levels, accumulated in leaf tissues in response to treatment with the flagellin  
315 epitope (flg22). At first, we studied callose accumulation in the absence of flg22 treatment  
316 (control; Fig. 3A). The *pi4kβ1β2* double mutant exhibited a constitutively high level of callose  
317 deposition, as previously shown (Antignani et al. 2015). We were able to show that a spatial  
318 pattern in callose accumulation existed, since the examination of different regions of interest  
319 (ROI) indicated a higher accumulation in the upper part of the leaf edges (Fig. 3B).

320 Callose accumulation was then assessed in either mock-infiltrated or flg22-treated plants  
321 (Fig.4). In this case, callose accumulation was much higher in *pi4kβ1β2* when compared to  
322 WT plants (Fig. 4A, B). The *sid2pi4kβ1β2* triple mutant was used to investigate whether high  
323 callose deposition in the double mutant depended on its high SA level. For mock treatments,  
324 callose deposition was much lower in *sid2pi4kβ1β2* compared to *pi4kβ1β2* plants. This  
325 provides arguments for a SA-dependent higher basal callose deposition. This was confirmed  
326 by the response to flg22. In WT plants, flg22 induced 20-times more callose compared to  
327 control mock infiltrations. Again, the callose level in *pi4kβ1β2* was higher (2-fold) compared  
328 to WT plants. This increase was reduced when the *sid2* mutation was introduced into the  
329 *pi4kβ1β2* double mutant as the level in the triple mutant was *circa* 2-fold lower than in the  
330 double mutant and in the same range as the WT level. This indicated that SA was a major  
331 inducer of callose accumulation in the *pi4kβ1β2* genotype context. Yet, the *sid2pi4kβ1β2*  
332 triple mutant exhibited a higher callose deposition than *sid2* plants. Therefore, the *pi4kβ1β2*  
333 double mutation *per se* had a role in the high callose accumulation observed in the *pi4kβ1β2*  
334 double mutant.

335 We also studied callose accumulation in leaf tissues in response to mechanical wounding (Fig.  
336 S4). Again, in response to wounding, the PI4K double mutation enhanced callose  
337 accumulation via a SA-dependent pathway.

338 Whether callose overaccumulation correlated with the transcription of callose synthases  
339 (*CalSs*) was then investigated. Among 12 callose synthases, *CalS1*, *CalS12* have been shown  
340 to be related to SA and/or biotic stresses (Dong et al. 2008). The transcript levels of *CalS1*  
341 and *CalS12* were tested by qPCR in WT, *pi4kβ1β2*, *sid2* and *sid2pi4kβ1β2* plants treated or  
342 not with flg22. No correlation was observed between *CalS1* and *CalS12* transcript levels and  
343 callose accumulation (Fig. S5).

344

#### 345 ***pi4kβ1β2* has altered non-host resistance that is SA-independent**

346 The establishment of non-host resistance is based on different mechanisms, involving  
347 vesicular secretion as well as callose accumulation (Collins et al. 2003, Assaad et al. 2004,  
348 Takemoto et al. 2006, Bohlenius et al. 2010, Lee et al., 2017). To study the role of PI4K in  
349 such responses, we tested penetration success and callose production in response to the non-  
350 host pathogen *Blumeria graminis* f. sp. *hordei* (*Bgh*). In *Bgh/A. thaliana* interactions, callose  
351 accumulates in defensive papillae and haustorial encasements or around dead cells (Assaad et  
352 al. 2004, Ellinger et al. 2013, Jacobs et al., 2003). The enhanced number of plant cells with  
353 developed haustoria or dead cells reflects the penetration success of fungal hyphae (Fig. 5A).  
354 In our experiments a higher penetration correlated with greater callose accumulation in the  
355 plant tissue. In particular the *pi4kβ1β2* double mutant showed an enhanced successful  
356 penetration of *Bgh* 24 h post inoculation (hpi), as seen by the enhanced number of haustoria  
357 and dead cells. A similar defect in penetration resistance was seen in *sid2/pi4kβ1β2*, thus  
358 revealing the SA-independent character of this phenomenon (Fig. 5B). Both, *pi4kβ1β2* and  
359 *sid2/pi4kβ1β2* accumulated more callose (Fig. 5C) and over larger areas compared to WT



360 plants (Fig. 5C, D). Thus, the lower penetration resistance accompanied by callose  
361 accumulation in *pi4kβ1β2* was independent of the SA pathway.

362

## 363 **DISCUSSION**

364 The aim of this study was to investigate SA-dependent and -independent processes caused by  
365 the *pi4kβ1β2* double mutation. As previously shown (Sasek et al. 2014), this mutant  
366 accumulates a constitutively high level of SA. In *pi4kβ1β2*, SA biosynthesis is dependent on  
367 ISOCHORISMATE SYNTHASE 1 (ICS1), demonstrated by an absence of SA accumulation  
368 in the *sid2pi4kβ1β2* triple mutant with impaired *ICS1* transcription (Sasek et al. 2014). This  
369 was confirmed with the hormone analysis described in the present study. The *sid2pi4kβ1β2*  
370 triple mutant lacking high SA was used as a tool to distinguish between SA-dependent and  
371 SA-independent effects caused by the double mutation in *pi4kβ1β2*.

372 We first measured phytohormonal levels in fully developed leaves of four-week-old *A.*  
373 *thaliana* WT, *pi4kβ1β2*, *sid2* and *sid2pi4kβ1β2* plants. According to our knowledge, this is  
374 the broadest phytohormonal study carried out with a SA over-accumulating mutant (in our  
375 case *pi4kβ1β2*) and its comparison with a plant having the same background but with an  
376 impaired SA pathway (*sid2pi4kβ1β2*). The level of 15 hormone derivatives (excluding SA)  
377 was altered in *pi4kβ1β2* compared to WT leaves. For 13 of these, this was SA-dependent. We  
378 could identify two metabolites, *cis*-zeatin-riboside-5'-monophosphate and glucosylesters of  
379 oxindole-3-acetic acid, for which the *pi4kβ1β2* double mutation effect was SA-independent.  
380 The same conclusions were also reached with another triple mutant, *NahGpi4kβ1β2*. Amongst  
381 the hormones controlled by SA were ABA derivatives such as DPA, PA and 9OH-ABA. As  
382 ABA levels did not correlate with SA, the action of SA on ABA-derivatives did not appear to  
383 act on ABA biosynthesis but on its metabolism. Such an effect of SA on ABA catabolism is  
384 poorly described. A slight induction of ABA 8'-hydroxylase expression was observed after a

385 24 h SA treatment of rice seedlings (Mega et al. 2015). In an *A. thaliana cpr22* mutant  
386 (*constitutive expressor of PR genes 22*), the increase of SA and ABA levels due to a high-low  
387 humidity shift was also followed by the SA-dependent expression of genes encoding ABA  
388 metabolising enzymes (Mosher et al. 2010).

389 Other hormones displaying a high correlation to SA were IAA-Asp and some cytokinins (SA  
390 positively controlled cZROG and tZOG and negatively controlled tZ7G and tZ9G). The  
391 pattern of IAA was different from that of IAA-ASP, suggesting that SA control of IAA-Asp  
392 was on aspartate conjugation. Aspartate conjugation is catalysed by GH3.2-GH3.6 (Normanly  
393 2010), with our transcriptome data obtained with *in vitro* grown *pi4kβ1β2* seedlings (Sasek et  
394 al. 2014) indicating that *GH3.3* (At2g23170) was overexpressed in the double mutant. It  
395 would be interesting to investigate whether it was responsible for the IAA-Asp/SA correlation  
396 in our double mutant.

397 Our results demonstrate the major role of hormonal cross-talk between SA and other  
398 hormones but only a minor role of impairment of PI4Kβ1/β2 *per se*. Since a major role of SA  
399 is related to responses to biotic stresses, we reasoned that other processes related to biotic  
400 stress, whether SA-dependent or not, could also be altered in the double mutant. We tested the  
401 resistance of WT, *pi4kβ1β2*, *sid2* and *sid2pi4kβ1β2* plants against representative biotrophic  
402 (oomycete *H. arabidopsidis* NoCo2), hemibiotrophic (bacteria *Pst* DC3000) and necrotrophic  
403 (fungus *B. cinerea*) pathogens. Results clearly showed that resistance to these pathogens was  
404 dependent on a high SA content. Resistance to *H. arabidopsidis* NoCo2 and *Pst* DC3000 was  
405 perhaps not surprising as resistance to such pathogens is generally associated with SA  
406 signalling (Glazebrook 2005). On the other hand, the role of SA in regulating resistance to  
407 necrotrophs is rather uncommon. Indeed, plant defence against necrotrophs is commonly  
408 associated with jasmonic acid signalling (Glazebrook 2005; Ferrari et al. 2003). However,  
409 Ferrari et al. (2003) showed that resistance to *B. cinerea* could be dependent on high SA

410 levels, in accordance with our observations. A similar finding was reported for defence  
411 response to the necrotroph *Sclerotinia sclerotiorum* (Novakova et al. 2014). Moreover, we  
412 tested *A. thaliana* ETI by using a bacterial strain highly expressing the AvrRpt2 effector (*Pst*  
413 DC3000 AvrRpt2). An ETI response can induce the expression of genes commonly associated  
414 with SA, such as *PR-1*, in a SA-independent manner in *A. thaliana* (Tsuda et al. 2013). Yet,  
415 we found that the higher resistance of *pi4kβ1β2* plants against *Pst* DC3000 AvrRpt2 was SA-  
416 dependent. In conclusion, the higher resistance of *pi4kβ1β2* mutant against all the host  
417 pathogens assayed was strongly SA-dependent.

418 Non-host resistance, efficient against non-adapted pathogens, does not rely fully on the SA  
419 pathway. Here we show that *pi4kβ1β2* exhibited a SA-independent defective resistance  
420 towards penetration of the non-host pathogen *Bgh*.

421 Callose is a linear polysaccharide (1,3-β-glucan) occurring in plant cells where it is important  
422 for many plant physiological processes such as cytokinesis (Chen and Kim 2009). Callose  
423 accumulation is triggered in response to pathogens and is used as a common test of PTI upon  
424 treatment with typical PAMPs such as flg22, the epitope of flagellin (Luna et al. 2011). In  
425 mock inoculated *pi4kβ1β2*, callose deposition was greater than in WT leaves, thus confirming  
426 findings of Antignani et al. (2015). Interestingly, this was also true for the *sid2pi4kβ1β2* triple  
427 mutant when compared to *sid2* plants, thus indicating a SA-independent phenomenon.  
428 Following inoculation with flg22, an increase in callose deposition was observed in all  
429 genotypes tested, but this was still higher in *pi4kβ1β2* compared to WT leaves, and callose  
430 deposition was higher in *sid2pi4kβ1β2* with respect to *sid2* plants. Therefore, it seems that the  
431 *pi4kβ1β2* double mutation *per se* enabled higher callose deposition under biotic stress  
432 conditions.

433 The biosynthesis of callose occurs outside of the cell (Ellinger and Voigt 2014).  
434 Accumulation can be regulated at different levels: transcriptional, translational, or during

435 enzyme transport to the plasma membrane and out of the cell via vesicular trafficking.  
436 Phosphorylation and direct translocation of callose synthase is crucial in the regulation of  
437 biosynthesis, whereas transcriptional control might have only a minor role (Ellinger and Voigt  
438 2014). Our data on the transcription levels of *CALS1* and *CALS12* indicate that in *pi4kβ1β2* a  
439 transcriptional effect is not involved in the observed over accumulation of callose. So how is  
440 it possible to explain the action on callose of the *pi4kβ1β2* double mutation *per se*? A number  
441 of reports indicate that PI4Ks can impact trafficking. In *A. thaliana*, PI4Kβ1 was shown to be  
442 recruited by the GTP bound Rab4b GTPase. Both RabA4b and PI4Kβ1 localize to budding  
443 secretory vesicles in the trans-golgi network (TGN) and to secretory vesicles *en route* to the  
444 cell surface. A *pi4kβ1β2* double mutant produces secretory vesicles of highly variable sizes  
445 (Antignani et al. 2015; Preuss et al. 2006; Kang et al. 2011). The product of PI4Ks activity,  
446 PI4P massively accumulates at the plasma membrane and at early endosomes / TGN and  
447 Golgi (Platre and Jaillais 2016; Noack and Jaillais 2017). Therefore PI4Kβ1/β2 are important  
448 in vesicle trafficking. Interestingly, inhibiting PI4K with phenylarsine oxide (PAO)  
449 suppressed the salt-induced endocytosis of plasma membrane intrinsic protein 2;1 (Ueda et  
450 al., 2016). Similarly, inhibiting PI4K led to the internalization of CELLULOSE  
451 SYNTHASE3 from the plasma membrane (Fujimoto et al. 2015). Can the impact of PI4K  
452 betas on trafficking explain the increased callose accumulation? Callose biosynthesis and  
453 accumulation have been shown to be affected by vesicle trafficking (Ellinger and Voigt  
454 2014). PI4Ks has been shown to play an important role in cytokinesis (Lin et al. 2019),  
455 especially in the correct organization of the vesicles at the cell division plane and further  
456 formation of a cell plate. During phragmoplast formation, PI4Kβ1 likely interacts with  
457 MPK4, a member of the MAP65 protein family that regulates microtubule organization (Lin  
458 et al., 2019). Callose is also essential for cytokinesis (Thiele et al. 2009). We can therefore  
459 only speculate whether the effects of PI4Ks on callose, cytokinesis and trafficking are

460 interconnected. Interestingly, the role of SA in these processes has not been tested. Since  
461 PI4K $\beta$ 1/ $\beta$ 2 can impact the secretory pathway, they could also impact the translocation of  
462 callose synthases. Furthermore, PMR4 (CALS12) binds to small RabA4c GTPase at TGN and  
463 PI4K $\beta$ 1 binds to RabA4b GTPase, the most similar small GTPase to RabA4c, at TGN  
464 (Böhlenius et al., 2010). It should also be noted that the impact of PI4K betas on trafficking  
465 could also explain our non-host resistance data. The *syp121* mutant altered in a SNARE  
466 protein involved in trafficking has been reported to accumulate SA and also display defective  
467 non-host resistance (Collins et al., 2003).

468

469 In conclusion (Fig. 6), the *pi4k $\beta$ 1 $\beta$ 2* double mutant constitutively accumulated a high SA  
470 level via ICS1/SID2 and this had a big impact on other hormone levels and it was associated  
471 with an increased resistance to several plant pathogens (*P. syringae*, *H. arabidopsidis*, *B.*  
472 *cinerea*). The *pi4k $\beta$ 1 $\beta$ 2* double mutation also affected pathogen-related processes in a high  
473 SA-independent manner as seen by differences in callose accumulation in response to *flg22*,  
474 to *Bgh* infection, to wounding, and the higher penetration success of *Bgh*. The identification  
475 of such processes directly affected by the mutation on PI4Ks will now allow us to better  
476 investigate the role of these enzymes, in relation to signalling or trafficking events.

477

478

479

480 **Funding information**

481 This work was supported by the Czech Science Foundation [grant number. 17-05151S].  
482 Collaboration of Ukrainian and French teams was partially supported by a “Projet  
483 international de coopération scientifique” from the “Centre National de la Recherche  
484 Scientifique” (2015-2018). TK received the Visegrad scholarship (2016-2017) [grant number  
485 51600349]; she also benefited from the Program of Postdoctoral Fellowships of the Czech  
486 Academy of Sciences [grant number TK 919220]. The work was also supported by a  
487 European Regional Development Fund-Project "Centre for Experimental Plant Biology"  
488 [grant number CZ.02.1.01/0.0/0.0/16\_019/0000738].

489

#### 490 **ACKNOWLEDGEMENTS**

491 We thank Lucie Lamparová and Romana Pospíchalová for their technical support and  
492 Michael Hodges for language editing.

493

#### 494 **LITERATURE CITED**

- 495 **Antignani V, Klocko AL, Bak G, Chandrasekaran SD, Dunivin T, Nielsen E.** 2015.  
496 Recruitment of PLANT U-BOX13 and the PI4Kbeta1/beta2 phosphatidylinositol-4  
497 kinases by the small GTPase RabA4B plays important roles during salicylic acid-  
498 mediated plant defense signaling in Arabidopsis. *Plant Cell*, **27**, 243-61.
- 499 **Assaad, F. F., Qiu, J. L., Youngs, H., Ehrhardt, D., Zimmerli, L., Kalde, M., ... &**  
500 **Somerville, C. R.** (2004). The PEN1 syntaxin defines a novel cellular compartment  
501 upon fungal attack and is required for the timely assembly of papillae. *Molecular*  
502 *biology of the cell*, 15(11), 5118-5129.
- 503 **Balla T.** 2007. Imaging and manipulating phosphoinositides in living cells. *Journal of*  
504 *Physiology*, **582**, 927–937.
- 505 **Böhlenius, H., Mørch, S. M., Godfrey, D., Nielsen, M. E., & Thordal-Christensen, H.**  
506 (2010). The multivesicular body-localized GTPase ARFA1b/1c is important for callose  
507 deposition and ROR2 syntaxin-dependent preinvasive basal defense in barley. *The*  
508 *Plant Cell*, tpc-110.

509 **Cao H, Glazebrook J, Clarke JD, Volko S, Dong X.** 1997. The Arabidopsis NPR1 gene that  
510 controls systemic acquired resistance encodes a novel protein containing ankyrin  
511 repeats. *Cell*, **88**, 57-63.

512 **Collins NC, Thordal-Christensen H, Lipka V, et al.** 2003. SNARE-protein-mediated  
513 disease resistance at the plant cell wall. *Nature*, **425**, 973-7.

514 **Cui H, Gobbato E, Kracher B, Qiu J, Bautor J, Parker JE.** 2017. A core function of EDS1  
515 with PAD4 is to protect the salicylic acid defense sector in Arabidopsis immunity.  
516 *New Phytologist*, **213**, 1802-1817.

517 **Czechowski T, Stitt M, Altmann T, Udvardi MK, Scheible WR.** 2005. Genome-wide  
518 identification and testing of superior reference genes for transcript normalization in  
519 Arabidopsis. *Plant Physiology*, **139**, 5-17.

520 **Delage E, Ruelland E, Guillas I, Zachowski A, Puyaubert J.** 2012. Arabidopsis type-III  
521 phosphatidylinositol 4-kinases beta1 and beta2 are upstream of the phospholipase C  
522 pathway triggered by cold exposure. *Plant and Cell Physiology*, **53**, 565-76.

523 **Delaney TP, Uknes S, Vernooij B, et al.** 1994. A central role of salicylic Acid in plant  
524 disease resistance. *Science*, **266**, 1247-50.

525 **Dobrev PI, Hoyerova K, Petrasek J.** 2017. Analytical Determination of Auxins and  
526 Cytokinins. *Methods in Molecular Biology*, **1569**, 31-39.

527 **Dobrev PI, Kaminek M.** 2002. Fast and efficient separation of cytokinins from auxin and  
528 abscisic acid and their purification using mixed-mode solid-phase extraction. *Journal*  
529 *of Chromatography A*, **950**, 21-9.

530 **Dobrev PI, Vankova R.** 2012. Quantification of abscisic Acid, cytokinin, and auxin content  
531 in salt-stressed plant tissues. *Methods in Molecular Biology*, **913**, 251-61.

532 **Dong X, Hong Z, Chatterjee J, Kim S, Verma DP.** 2008. Expression of callose synthase  
533 genes and its connection with Npr1 signaling pathway during pathogen infection.  
534 *Planta*, **229**, 87-98.

535 **Ellinger D, Glockner A, Koch J, et al.** 2014. Interaction of the Arabidopsis GTPase RabA4c  
536 with its effector PMR4 results in complete penetration resistance to powdery mildew.  
537 *Plant Cell*, **26**, 3185-200.

538 **Ellinger D, Voigt CA.** 2014. Callose biosynthesis in Arabidopsis with a focus on pathogen  
539 response: what we have learned within the last decade. *Annals of Botany*, **114**, 1349-  
540 58.

541 **Ferrari S, Plotnikova JM, De Lorenzo G, Ausubel FM.** 2003. Arabidopsis local resistance  
542 to Botrytis cinerea involves salicylic acid and camalexin and requires EDS4 and  
543 PAD2, but not SID2, EDS5 or PAD4. *Plant Journal*, **35**, 193-205.

544 **Fujimoto M, Suda Y, Vernhettes S, Nakano A, Ueda T.** 2015. Phosphatidylinositol 3-  
545 kinase and 4-kinase have distinct roles in intracellular trafficking of cellulose synthase  
546 complexes in Arabidopsis thaliana. *Plant and Cell Physiology*, **56**, 287-98.

547 **Glazebrook J.** 2005. Contrasting mechanisms of defense against biotrophic and necrotrophic  
548 pathogens. *Annual Review of Phytopathology*, **43**, 205-27.

549 **Gross J, Cho WK, Lezhneva L, et al.** 2006. A plant locus essential for phylloquinone  
550 (vitamin K1) biosynthesis originated from a fusion of four eubacterial genes. *Journal*  
551 *of Biological Chemistry*, **281**, 17189-96.

552 **Chen XY, Kim JY.** 2009. Callose synthesis in higher plants. *Plant Signaling and Behaviour*,  
553 **4**, 489-92.

554 **Jacobs AK, Lipka V, Burton RA, et al.** 2003. An Arabidopsis callose synthase, GSL5, is  
555 required for wound and papillary callose formation. *Plant Physiology*, **15**, 2503-2313.

556 **Janda M, Sasek V, Ruelland E.** 2014. The Arabidopsis pi4kIIIbeta1beta2 double mutant is  
557 salicylic acid-overaccumulating: a new example of salicylic acid influence on plant  
558 stature. *Plant Signaling and Behaviour*, **9**, e977210.



559 **Janda M, Ruelland E.** 2015. Magical mystery tour: salicylic acid signalling. *Environmental*  
560 *and Experimental Botany*, **114**, 117-128.

561 **Kalachova T, Puga-Freitas R, Kravets V, et al.** 2016. The inhibition of basal  
562 phosphoinositide-dependent phospholipase C activity in Arabidopsis suspension cells  
563 by abscisic or salicylic acid acts as a signalling hub accounting for an important  
564 overlap in transcriptome remodelling induced by these hormones. *Environmental and*  
565 *Experimental Botany*, **123**, 37-49.

566 **Kang BH, Nielsen E, Preuss ML, Mastrorarde D, Staehelin LA.** 2011. Electron  
567 tomography of RabA4b- and PI-4Kbeta1-labeled trans Golgi network compartments in  
568 Arabidopsis. *Traffic*, **12**, 313-29.

569 **Katagiri F, Thilmony R, He SY.** 2002. The Arabidopsis thaliana-pseudomonas syringae  
570 interaction. *Arabidopsis Book*, **1**, e0039.

571 **Kohler A, Schwindling S, Conrath U.** 2002. Benzothiadiazole-induced priming for  
572 potentiated responses to pathogen infection, wounding, and infiltration of water into  
573 leaves requires the NPR1/NIM1 gene in Arabidopsis. *Plant Physiology*, **128**, 1046-56.

574 **Krinke O, Ruelland E, Valentová O, et al.** 2007. Phosphatidylinositol 4-Kinase activation is  
575 an early response to salicylic acid in Arabidopsis suspension cells. *Plant Physiology*,  
576 **144**, 1347-1359.

577 **Krinke O, Flemr M, Vergnolle C, et al.** 2009. Phospholipase D activation is an early  
578 component of the salicylic acid signaling pathway in Arabidopsis cell suspensions.  
579 *Plant Physiology*, **150**, 424-36.

580 **Lee H-A, Lee H-Y, Seo E, et al.** 2017. Current understandings of plant Nonhost Resistance.  
581 *Molecular Plant-Microbe interactions*, **30**, 5-15

582 **Lin F, Krishnamoorthy P, Schubert V, et al.** 2019. A dual role for cell plate-associated  
583 PI4K $\beta$  in endocytosis and phragmoplast dynamics during plant somatic cytokinesis.  
584 The EMBO journal, e100303.

585 **Luna E, Pastor V, Robert J, Flors V, Mauch-Mani B, Ton J.** 2011. Callose deposition: a  
586 multifaceted plant defense response. *Molecular Plant-Microbe Interactions*, **24**, 183-  
587 93.

588 **Mega R, Meguro-Maoka A, Endo A, et al.** 2015. Sustained low abscisic acid levels increase  
589 seedling vigor under cold stress in rice (*Oryza sativa* L.). *Scientific Reports*, **5**, 13819.

590 **Mosher S, Moeder W, Nishimura N, et al.** 2010. The lesion-mimic mutant cpr22 shows  
591 alterations in abscisic acid signaling and abscisic acid insensitivity in a salicylic acid-  
592 dependent manner. *Plant Physiology*, **152**, 1901-13.

593 **Nakanishi S, Catt KJ, Balla T.** 1995. A wortmannin-sensitive phosphatidylinositol 4-kinase  
594 that regulates hormone-sensitive pools of inositolphospholipids. *Proceedings of the*  
595 *National Academy of Sciences of the USA*, **92**, 5317–5321.

596 **Noack LC, Jaillais Y.** 2017. Precision targeting by phosphoinositides: how PIs direct  
597 endomembrane trafficking in plants. *Current Opinion in Plant Biology*, **40**, 22-33.

598 **Normanly J.** 2010. Approaching cellular and molecular resolution of auxin biosynthesis and  
599 metabolism. *Cold Spring Harbor Perspectives in Biology*, **2**, a001594.

600 **Novakova M, Sasek V, Dobrev PI, Valentova O, Burketova L.** 2014. Plant hormones in  
601 defense response of *Brassica napus* to *Sclerotinia sclerotiorum* - reassessing the role of  
602 salicylic acid in the interaction with a necrotroph. *Plant Physiol Biochem*, **80**, 308-17.

603 **Pappan K, Austin-Brown S, Chapman KD, Wang X.** 1998. Substrate selectivities and lipid  
604 modulation of plant phospholipase D alpha, -beta, and -gamma. *Archives of*  
605 *Biochemistry and Biophysics*, **353**, 131-40.

606 **Platre MP, Jaillais Y.** 2016. Guidelines for the Use of Protein Domains in Acidic  
607 Phospholipid Imaging. *Methods in Molecular Biology*, **1376**, 175-94.

608 **Preuss ML, Schmitz AJ, Thole JM, Bonner HK, Otegui MS, Nielsen E.** 2006. A role for  
609 the RabA4b effector protein PI-4Kbeta1 in polarized expansion of root hair cells in  
610 *Arabidopsis thaliana*. *Journal of Cell Biology*, **172**, 991-8.

611 **Sasek V, Janda M, Delage E, et al.** 2014. Constitutive salicylic acid accumulation in  
612 pi4kIIIbeta1beta2 *Arabidopsis* plants stunts rosette but not root growth. *New*  
613 *Phytologist*, **203**, 805-16.

614 **Seyfferth C, Tsuda K.** 2014. Salicylic acid signal transduction: the initiation of biosynthesis,  
615 perception and transcriptional reprogramming. *Frontiers in Plant Science*, **5**, 697.

616 **Takemoto, D., Jones, D. A., & Hardham, A. R.** (2006). Re-organization of the cytoskeleton  
617 and endoplasmic reticulum in the *Arabidopsis* pen1-1 mutant inoculated with the non-  
618 adapted powdery mildew pathogen, *Blumeria graminis f. sp. hordei*. *Molecular plant*  
619 *pathology*, 7(6), 553-563.

620 **Team RC.** 2014. R: A language and environment for statistical computing. R Foundation for  
621 Statistical Computing. *Vienna, Austria*.

622 **Thiele K, Wanner G, Kindzierski V, et al.** 2009. The timely deposition of callose is  
623 essential for cytokinesis in *Arabidopsis*. *The Plant Journal*, 58(1), 13-26.

624 **Tsuda K, Mine A, Bethke G, et al.** 2013. Dual regulation of gene expression mediated by  
625 extended MAPK activation and salicylic acid contributes to robust innate immunity in  
626 *Arabidopsis thaliana*. *PLoS Genetics*, **9**, e1004015.

627 **Vlot AC, Dempsey DA, Klessig DF.** 2009. Salicylic Acid, a Multifaceted Hormone to  
628 Combat Disease. *Annual Review of Phytopathology*, **47**, 177-206.

629 **Vogel J, Somerville S.** 2000. Isolation and characterization of powdery mildew-resistant  
630 *Arabidopsis* mutants. *Proceedings of the National Acadademy of Sciences U S A*, **97**,  
631 1897-902.

632 **Voigt CA.** 2014. Callose-mediated resistance to pathogenic intruders in plant defense-related  
633 papillae. *Frontiers in Plant Science*, **5**, 168.

634 **Wagner S, Stuttmann J, Rietz S, et al.** 2013. Structural Basis for Signaling by Exclusive  
635 EDS1 Heteromeric Complexes with SAG101 or PAD4 in Plant Innate Immunity. *Cell*  
636 *Host & Microbe*, **14**, 619-630.

637 **Wildermuth MC, Dewdney J, Wu G, Ausubel FM.** 2001. Isochorismate synthase is  
638 required to synthesize salicylic acid for plant defence. *Nature*, **414**, 562-5.

639 **Yi SY, Shirasu K, Moon JS, Lee SG, Kwon SY.** 2014. The activated SA and JA signaling  
640 pathways have an influence on flg22-triggered oxidative burst and callose deposition.  
641 *PLoS One*, **9**, e88951.

642 **Zhang Z, Feechan A, Pedersen C, et al.** 2007. A SNARE-protein has opposing functions in  
643 penetration resistance and defence signalling pathways. *Plant Journal*, **49**, 302-12.

644

## 645 **FIGURE CAPTIONS**

646 **Figure 1. Correlation matrix between phytohormones levels.** The matrix was built using  
647 the Pearson correlation of 27 hormone-related metabolites from 24 independent samples  
648 corresponding to 6 genotypes (WT; *sid2*; *NahG*; *pi4kβ1β2*; *sid2pi4kβ1β2*; *NahGpi4kβ1β2*;  
649 four plants per genotype). Positive correlations are displayed in blue and negative correlations  
650 in red. Colour intensity and the size of the circles are proportional to the correlation  
651 coefficients. Red rectangles highlight the correlation between SA and other hormones.

652

653 **Figure 2.** Resistance to biotic stresses of *pi4kβ1β2* and *sid2pi4kβ1β2* mutants. A. Resistance  
654 to biotroph *H. arabidopsidis*. B. Resistance to hemibiotroph *Pseudomonas syringae* pv.  
655 *syringae* DC3000. Infiltration treatment of 4 week-old-plants, with 6 independent samples. C.

656 Resistance to the necrotroph *Botrytis cinerea*. 4-5-week-old *A. thaliana* were inoculated with  
657 a 6  $\mu$ L drop containing spores of *B. cinerea* (50000 spores per mL), placed into a plastic box  
658 and kept in the dark for 56 h. Statistical differences between the genotypes for B and C were  
659 assessed using ANOVA, with a Tukey honestly significant difference (HSD) multiple mean  
660 comparison *post hoc* test. Different letters indicate a significant difference, Tukey HSD,  
661  $P < 0.05$ ,  $n=10$  for A,  $n=7$  for B and  $n=27$  for C.

662

663 **Figure 3. Pattern of callose accumulation in *pi4k $\beta$ 1 $\beta$ 2* leaves.** A. Aniline blue staining, and  
664 fluorescent microscopy. The bar corresponds to 500  $\mu$ m. B. Callose particles accumulated in  
665 different ROI. The squares represent the ROI. Data are presented as means  $\pm$ SEM. Statistical  
666 differences were assessed using a two-way ANOVA, with a Tukey honestly significant  
667 difference (HSD) multiple mean comparison *post hoc* test. Different letters indicate a  
668 significant difference, Tukey HSD,  $P < 0.05$ .  $n=11$ .

669

670 **Figure 4.** Callose deposition in response to flagellin. A. Representative images of callose  
671 accumulated in leaves of 4-week-old *A. thaliana* plants by aniline blue staining, 24 h after  
672 infiltration with 0.1  $\mu$ M flg22 or mock infiltration. The bar = 1cm. B. Quantification of  
673 callose particles. Values represent an average of 5 ROI. Data are presented as means +SD.  
674 For each treatment, statistical differences between the genotypes were assessed using a one-  
675 way ANOVA, with a Tukey honestly significant difference (HSD) multiple mean comparison  
676 *post hoc* test. Different letters indicate a significant difference, Tukey HSD,  $P < 0.01$ ,  $n=4$ .

677

678

679 **Figure 5.** Resistance of *pi4k $\beta$ 1 $\beta$ 2* to penetration by the non-host pathogen *Blumeria graminis*  
680 f. sp. *Hordei* (*Bgh*). A. Four types of interactions counted in the penetration success analysis

681 after trypan blue staining. Scale bar represents 5  $\mu\text{m}$ . B. Data showing penetration success of  
682 *Bgh* 24 hpi in each genotype, the mean number of cells with either haustoria or dead cells,  
683 respectively. C. Data show mean area of a callose spot per  $\text{mm}^2$  at 24hpi after interaction with  
684 *Bgh* spores. D. Data show mean area of a callose spot per  $\text{mm}^2$  at 24hpi after interaction with  
685 *Bgh* spores. Data at B, C and D were processed by ANOVA, with a Tukey honestly  
686 significant difference (HSD) multiple mean comparison *post hoc* test, the data represent 1  
687 independent experiment, the experiment was repeated four times. The letters indicate  
688 significant difference Tukey HSD,  $P < 0.01$ . E. Pictures demonstrating callose staining with  
689 aniline blue 24 hpi with *Bgh*. Scale bar 100  $\mu\text{m}$ .

690

691 **Figure 6.** Schematic representation of the effects of the *pi4k $\beta$ 1 $\beta$ 2* double mutation on  
692 Arabidopsis plants.

693

694

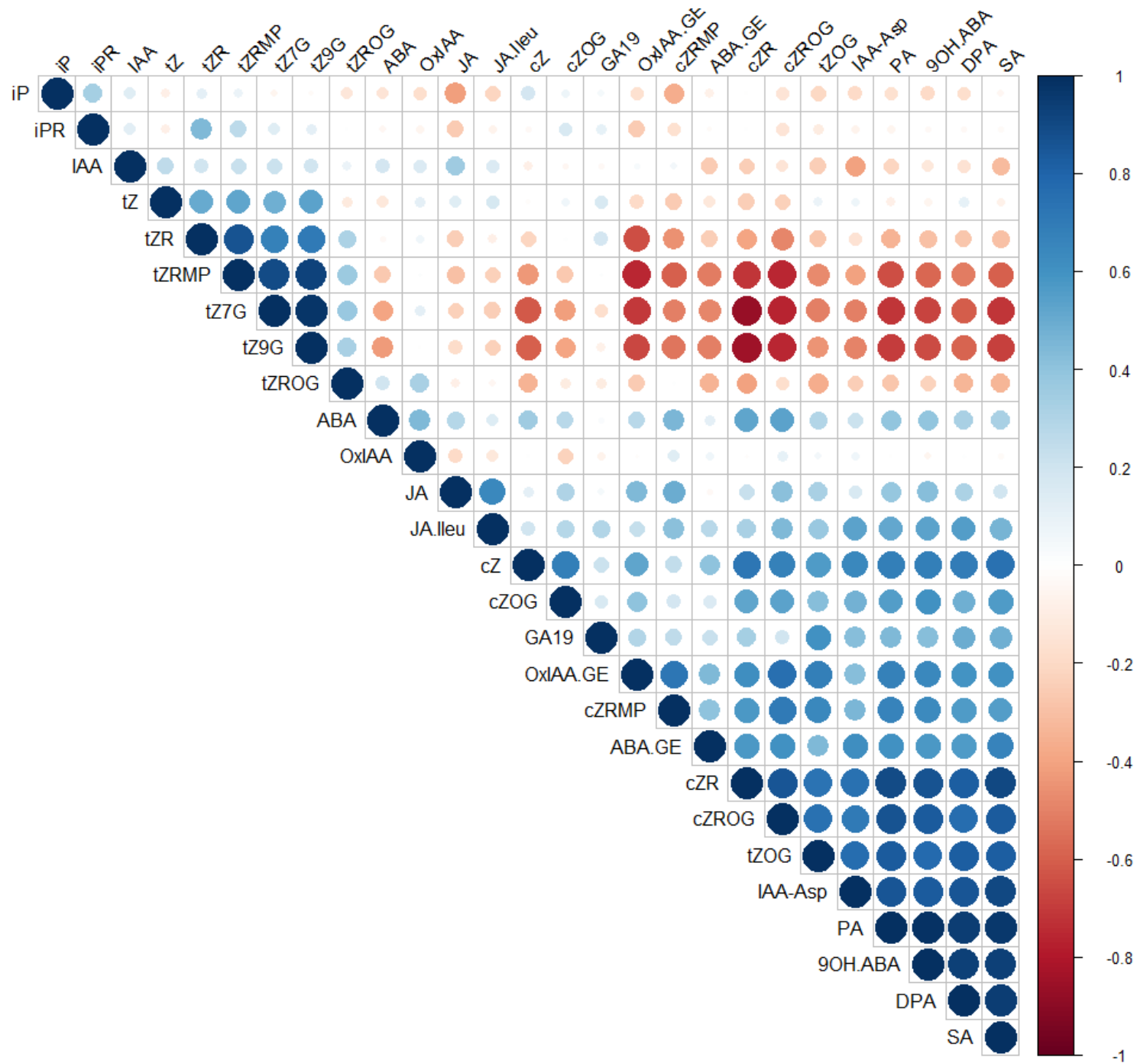
#### 695 **SUPPLEMENTARY DATA**

696 Supplemental Table S1. Phytohormone levels in 4-week-old plants. Values are expressed in  
697 pmol/gFW. For each genotype, 4 plants were assessed.

698 Fig. S1: Levels of hormones controlled by SA in four-week-old mutant and WT plants.  
699 Values represent means and SEM from four samples. For each hormone, statistical  
700 differences between the genotypes were assessed using a one-way ANOVA, with a Tukey  
701 honestly significant difference (HSD) multiple mean comparison *post hoc* test. Different  
702 letters indicate a significant difference, Tukey HSD,  $P < 0.05$ .  $n=4$ . Note the broken y-axis  
703 due to high SA in the *npr1pi4k $\beta$ 1 $\beta$ 2* triple mutant.

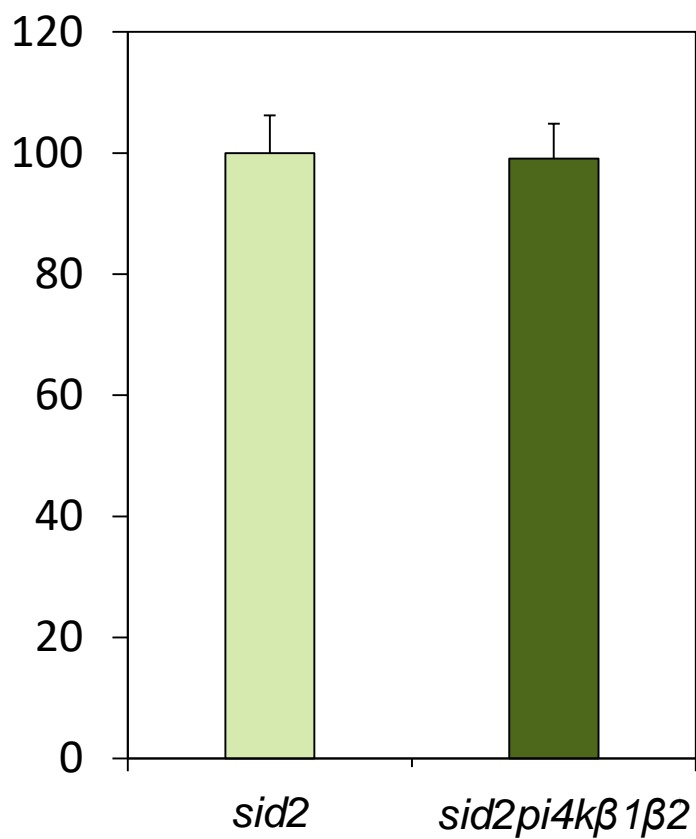
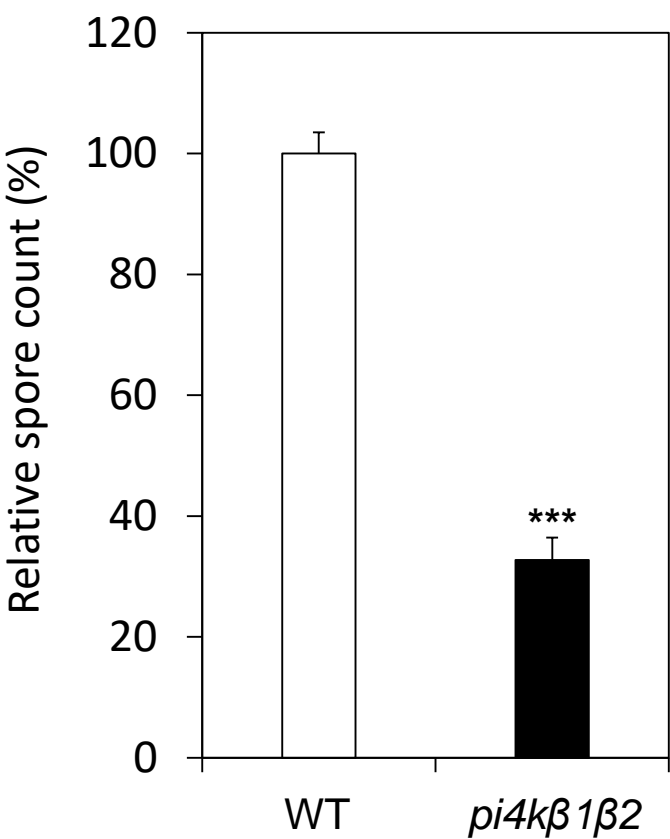
704 Fig. S2. Levels of hormones not controlled by SA in four-week-old mutant and WT plants.  
705 For each hormone, statistical differences between the genotypes were assessed using a one-

706 way ANOVA, with a Tukey honestly significant difference (HSD) multiple mean comparison  
707 *post hoc* test. Different letters indicate a significant difference, Tukey HSD,  $P < 0.05$ .  $n=4$ .  
708 Fig. S3. Resistance to *P. syringae* pv. *tomato* DC3000 AvrRpt2. 4-week-old *A. thaliana*  
709 plants were infiltrated with a bacterial suspension. Data show infection development at 2 dpi.  
710 Fig. S4. Callose deposition in response to wounding. A. Representative images of callose  
711 accumulated in leaves of 4-week-old *A. thaliana* plants 24 h after infiltration with a needleless  
712 syringe, leaf area outside of the place of infiltration (“mock”) or at the very place of treatment  
713 (“wounding”). Aniline blue staining, bar=1cm. B. Quantification of callose particles. Data are  
714 given as means +SD. For each treatment, statistical differences between the genotypes were  
715 assessed using a one-way ANOVA, with a Tukey honestly significant difference (HSD)  
716 multiple mean comparison *post hoc* test. Different letters indicate a significant difference,  
717 Tukey HSD,  $P < 0.01$ ,  $n=4$ .  
718 Fig. S5. Relative transcription of some *CalS* genes in untreated rosette leaves or 24h after  
719 infiltration with 0.1 $\mu$ M flg22.

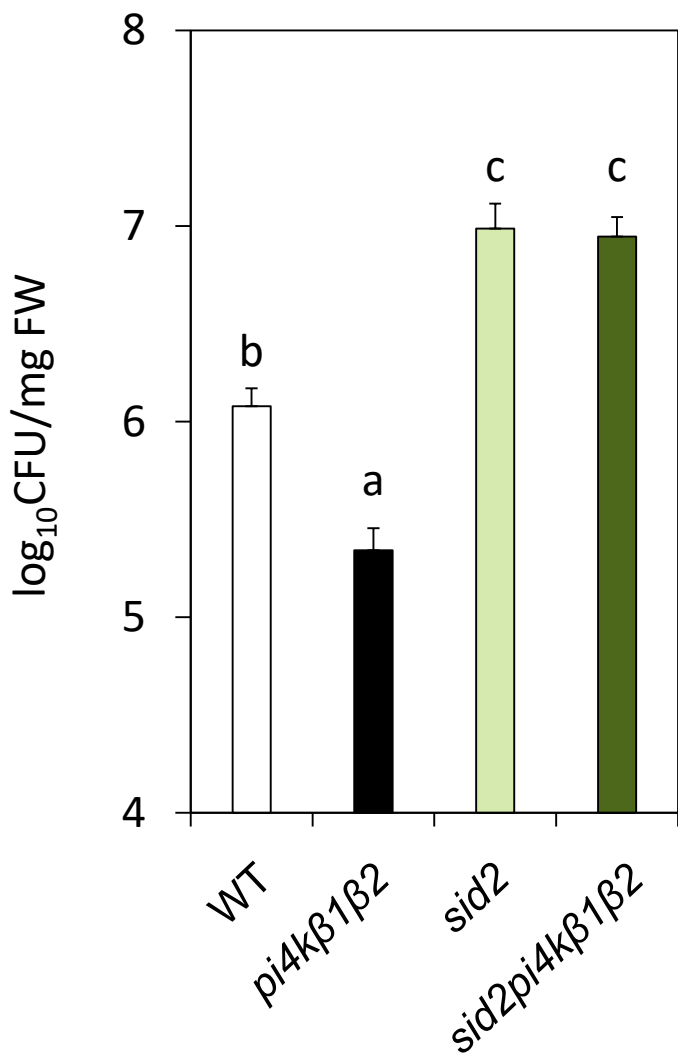




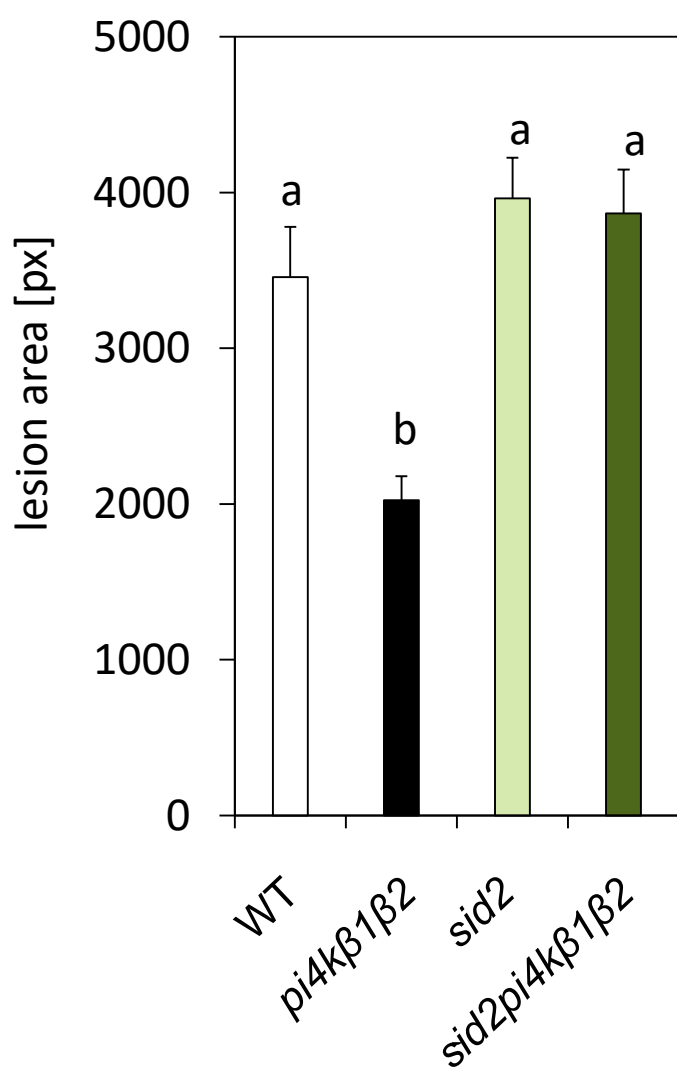
A. *H. arabidopsis*

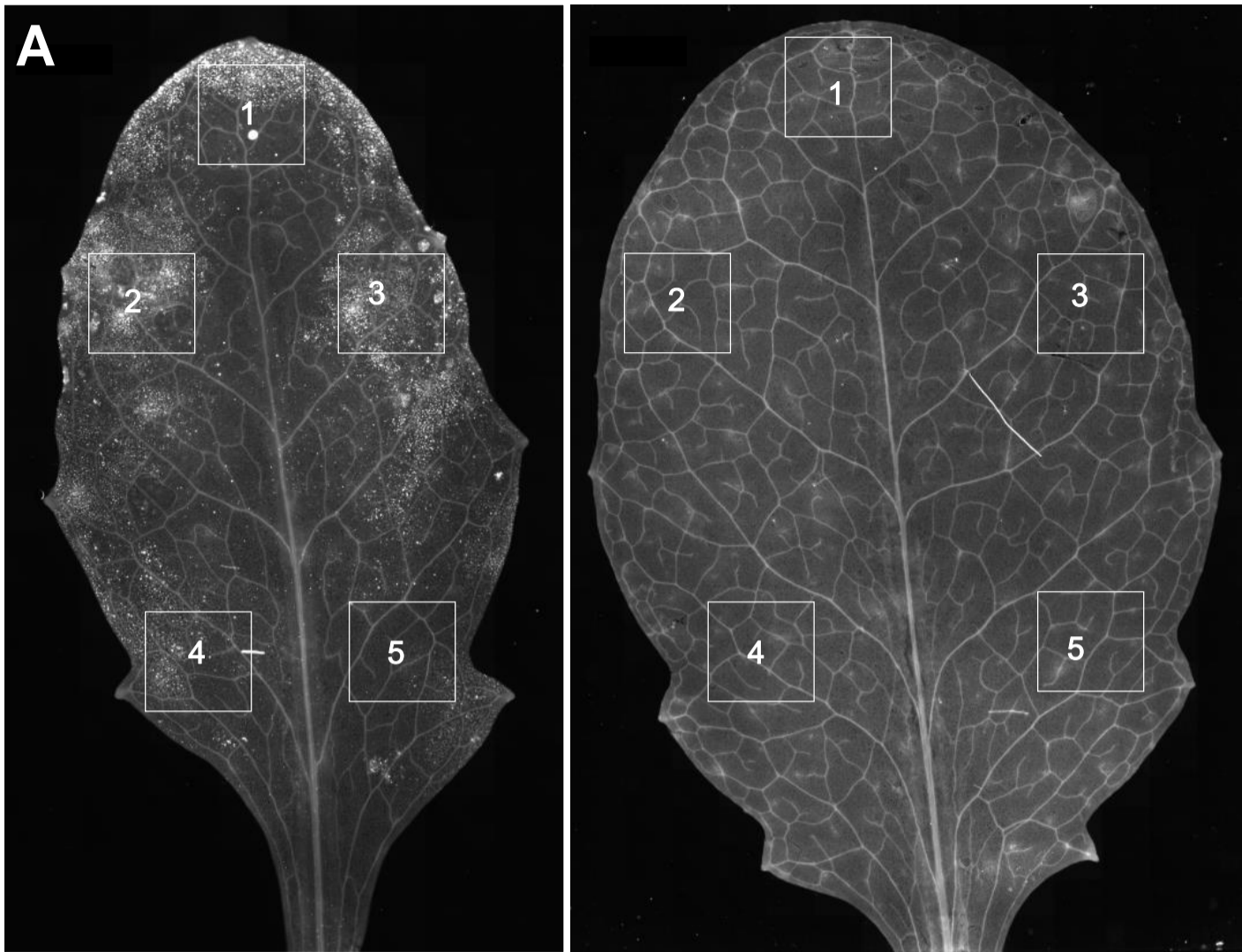


B. *Pst DC3000*



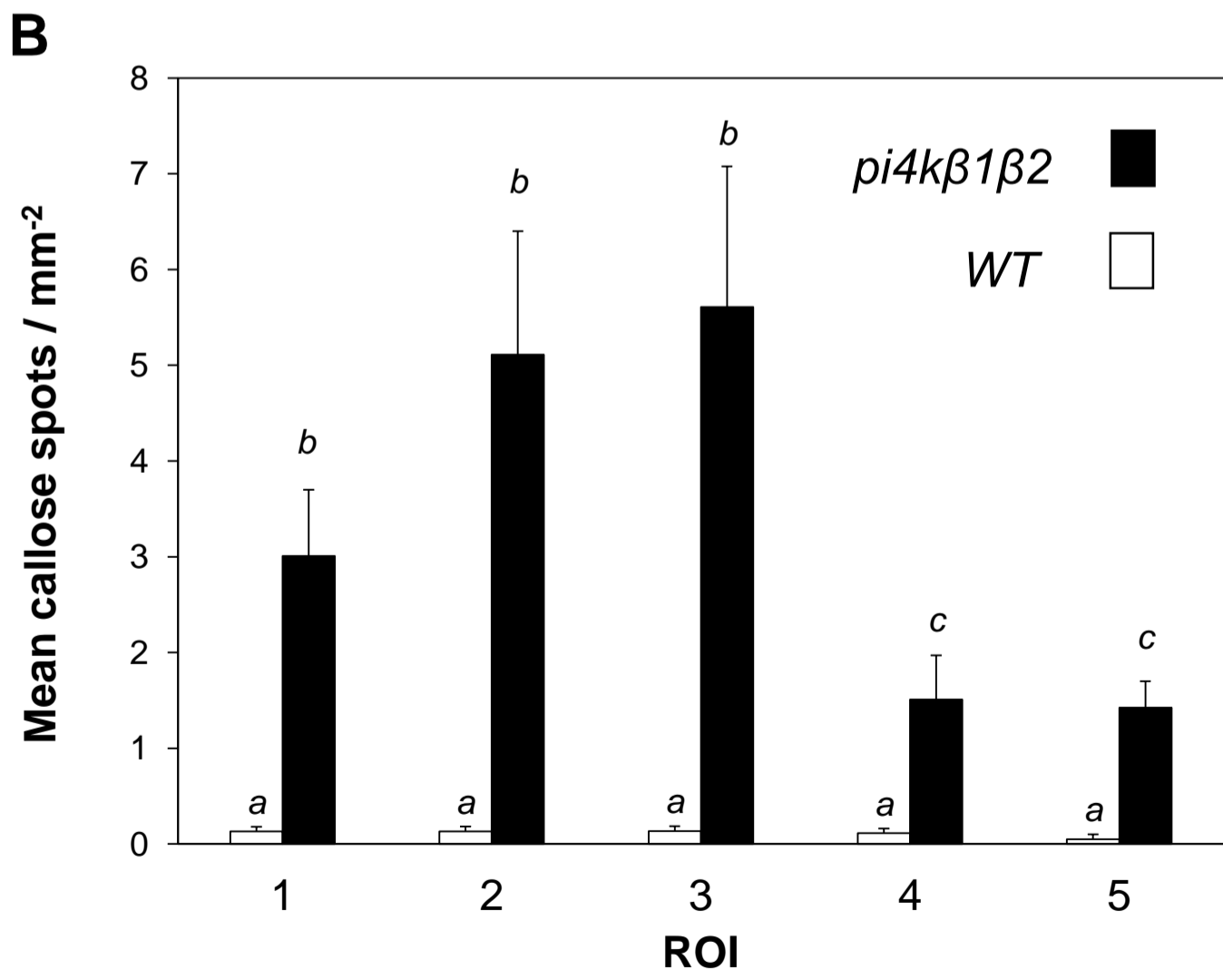
C. *B. cinerea*

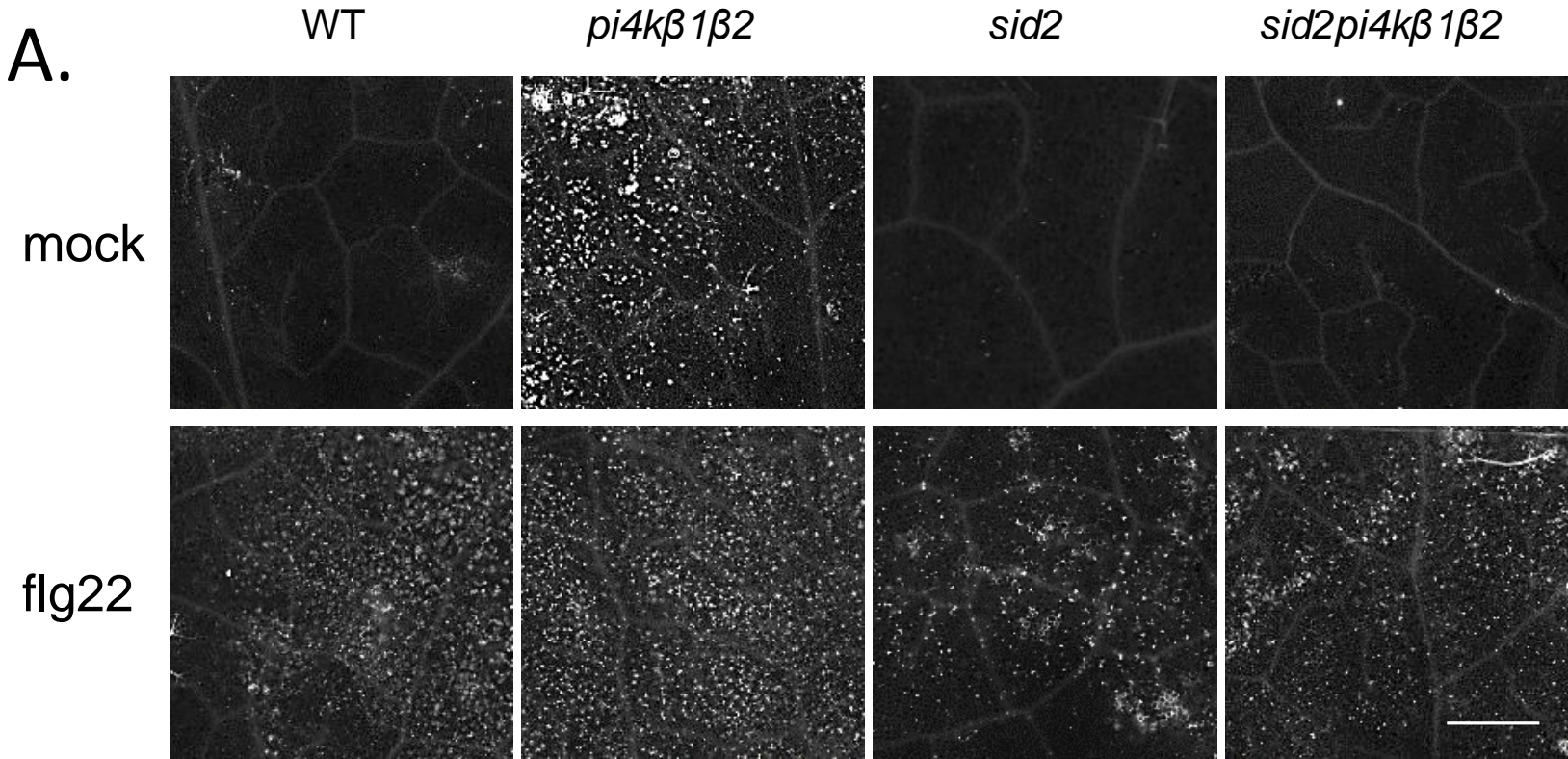




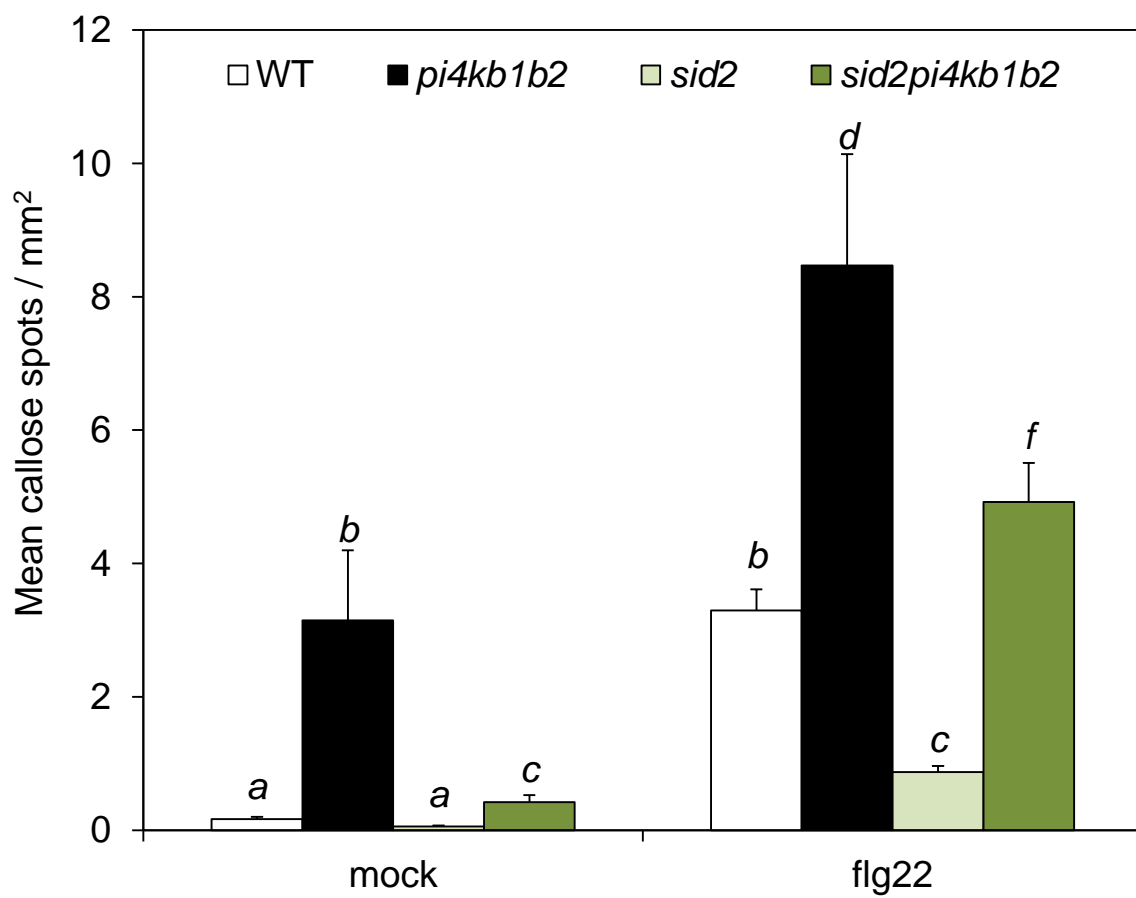
*pi4kβ1β2*

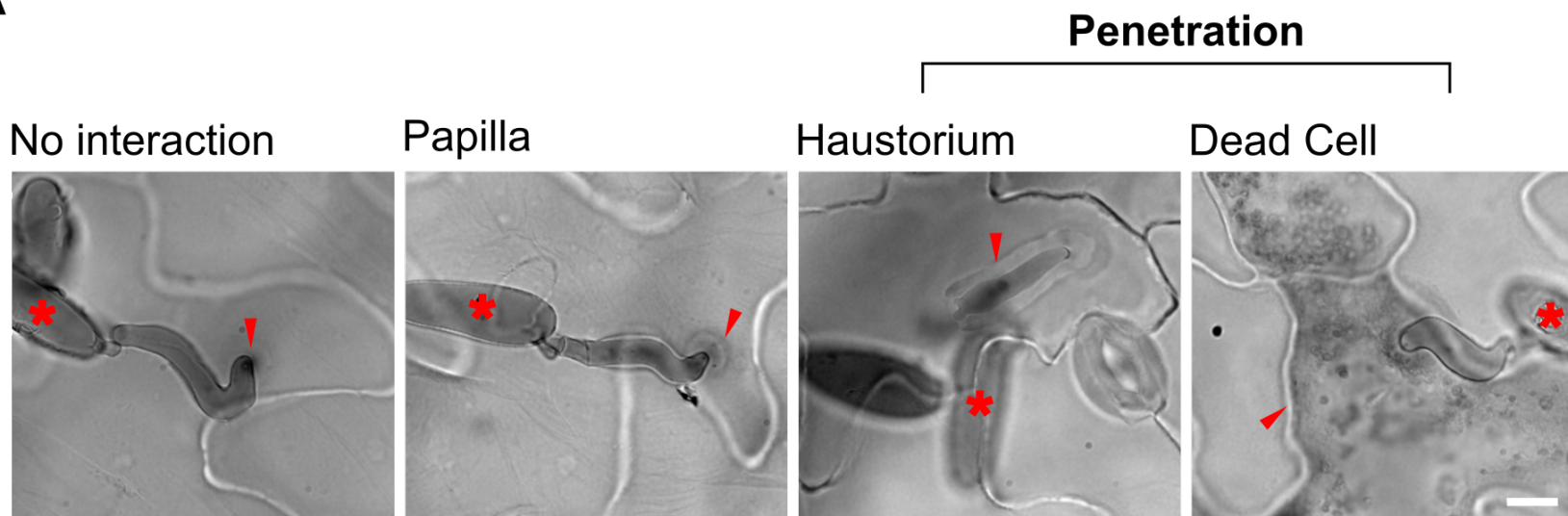
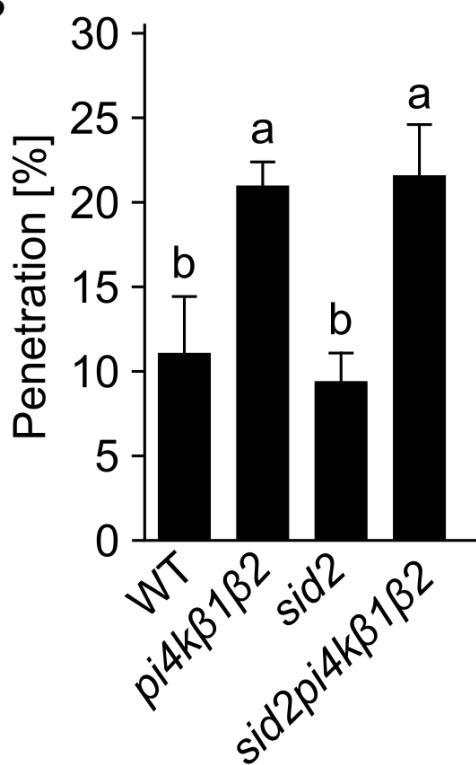
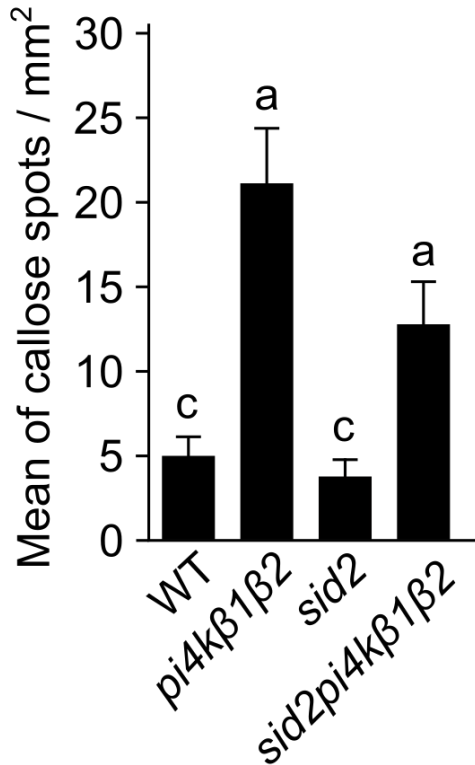
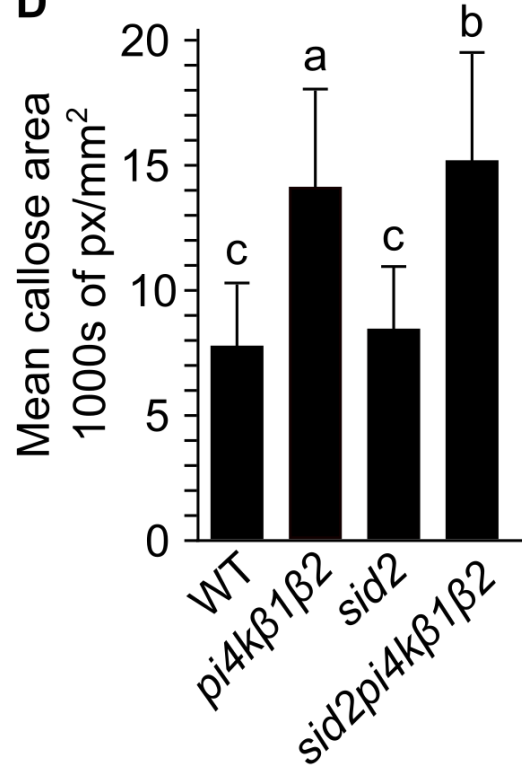
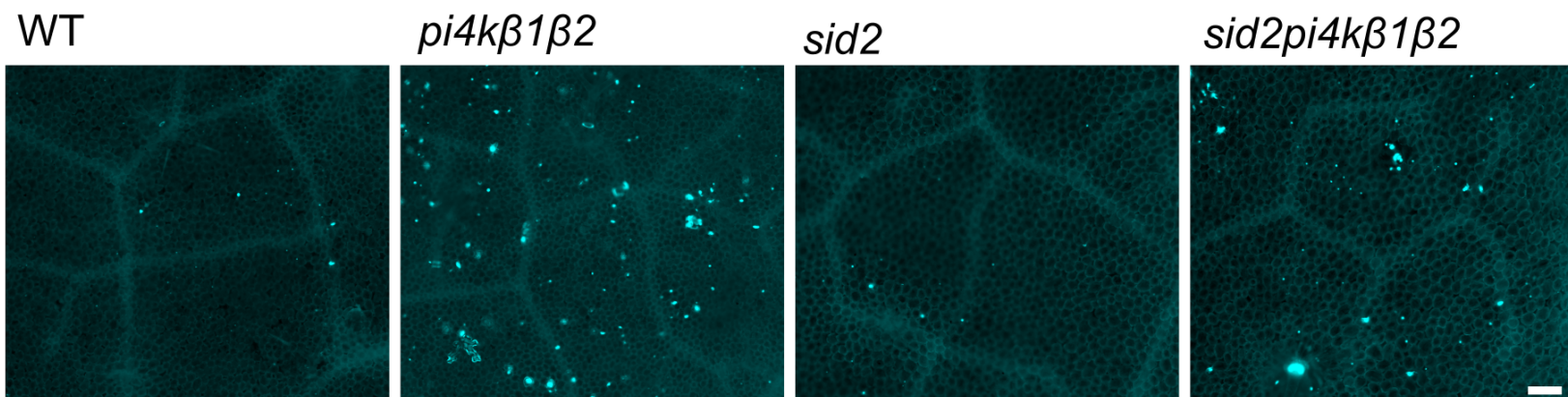
*WT*





**B.**



**A****B****C****D****E**

Hormonal cross-talk

